Ab initio investigations of magnetic properties of FeCo monolayer alloy films on Rh(001)

S. Blizak,[1,*] G. Bihlmayer,[2,†] and S. Blügel[2]

[1]*University M'Hamed Bougara of Boumerdés (UMBB), Unité de Recherche Matériaux Procédés et Environnement (ex: LMMC), 35000 Boumerdés, Algeria*

[2]*Peter Grünberg Institut and Institute for Advanced Simulation, Forschungszentrum Jülich and JARA, 52425 Jülich, Germany*

(Received 6 July 2012; published 28 September 2012)

The objective of this work is to employ spin-polarized density functional theory (sDFT) calculations for the exploration of ultrathin magnetic films with large magnetic moments and a strong perpendicular anisotropy. Monolayer films of $Fe_{1-x}Co_x$ (with $x = 0$, 0.25, 0.5, 0.75, and 1) on Rh(001) were addressed to study their magnetic properties using the all-electron full-potential linearized augmented plane wave (FLAPW) method in film geometry. We studied the magnetic order of these films including structural relaxations of the topmost layers. $Fe_{1-x}Co_x$ monolayer films were found to be ferromagnetic (FM) in a broad range of Co content x with a maximum magnetic moment of 2.8 μ_B and of an out-of-plane magneto-crystalline anisotropy of 0.25 meV per magnetic atom at $x = 0.5$. The sDFT results were mapped onto a classical Heisenberg model, demonstrating FM Fe-Co and Co-Co couplings, while the Fe-Fe interaction is antiferromagnetic on Rh(001). The ordering temperature of the FeCo film was estimated to be well above room temperature (482 K).

DOI: 10.1103/PhysRevB.86.094436 PACS number(s): 75.70.Ak, 73.20.−r, 71.15.Mb

I. INTRODUCTION

Materials with large magnetic moments and a strong perpendicular anisotropy are of great interest for information technology and recording media applications as well as magnetic field sensors.[1] In recent research, a great deal of attention has been devoted to transition-metal (TM) alloy films on various substrates. The $(Fe_{1-x}Co_x)_N$/Rh(001) system is an important example, since films on Rh(001)[2,3] show a perpendicular anisotropy up to $N = 15$ ML in a broad composition range (with a maximum value around $x = 0.5$) even at room temperature.[4] 3*d* transition metal monolayers on rhodium substrate have been systematically investigated within *ab initio* calculations in Ref. 5: The magnetic order was found to be ferromagnetic for Co whereas Fe favors an antiferromagnetic (AFM) ground state. In addition, calculations of the magnetic anisotropy energy (MAE) showed that the magnetization of both Fe and Co is oriented in-plane. Therefore, we address the following question: What happens when we take both iron and cobalt with a certain concentration? The answer to this question can be anticipated through the extensive experimental work realized by Yildiz and collaborators. In Ref. 2 they studied tetragonally distorted $Fe_{1-x}Co_x$ alloy films on Rh(001) which show a strong perpendicular anisotropy in a wide thickness (up to 15 ML) and composition range (i.e., Co content of $0.3 < x < 0.6$). Theoretically, for FeCo alloys the stability of the cubic bulk phase as function of the concentration was investigated in Ref. 6 where a partially ordered B2 phase was predicted in a large concentration range. At the Rh(001) lattice constant tetragonalization has been predicted for Fe films[7] and for films on Rh(001) with a few layer thickness this was confirmed, also significantly affecting the magnetic ordering of the layers.[8] However, for tetragonalized (bulk) FeCo alloys large perpendicular anisotropies were found,[9] rendering this material useful for practical applications. These findings motivate a more systematic investigation of 3*d* transition-metal alloy films on the Rh(001) substrate. In this paper we investigate the magnetic properties of (ordered) $Fe_{1-x}Co_x$ alloy monolayers on Rh(001) for $x = 0.0, 0.25, 0.5, 0.75$, and 1.0. In Sec. II we outline the computational method, while in Sec. III we study the relaxations of the topmost layers, the magnetic order and moments, and the magnetic anisotropy and orbital moments, and we finally conclude with a summary in Sec. IV.

II. COMPUTATIONAL DETAILS

Thin films of $Fe_{1-x}Co_x$ on Rh(001) were addressed to study their magnetic properties using spin density functional theory (sDFT).[10–12] All calculations in this work were made using the FLEUR[13] implementation of the all-electron full-potential linearized augmented plane wave (FLAPW) method[14] in film geometry.[15] The generalized gradient approximation to the exchange-correlation functional of Perdew *et al.* is used.[16] Spin-orbit interactions were considered via a second variational step using the scalar-relativistic eigenfunctions as a basis.[17] The films are modeled by a symmetric seven-layer Rh(001) slab covered by 3*d* transition-metal monolayers (ML) on each side, using the calculated Rh in-plane lattice constant 3.819 Å in Ref. 5. The plane wave (PW) cutoff parameter is chosen as $k_{max} = 7.56$ Å^{-1} with a muffin-tin sphere radius of $R_{MT} = 1.22$ Å for the 3*d* atoms and 1.28 Å for the Rh atoms.

III. $Fe_{1-x}Co_x$ MONOLAYER ON Rh(001)

A. Relaxations

Relaxations were considered for the topmost two layers, that is, the 3*d* ML and the interface layer Rh(I) (see Fig. 1). The number of $\mathbf{k}_\parallel$ points used in the irreducible Brillouin zone (IBZ) were up to 78 for the $c(2 \times 2)$ surface unit cell and 15 for the $p(2 \times 2)$ configuration. The relative relaxations between the layers i and j are characterized by

$$\Delta d_{ij} = \frac{d_{ij} - d_0}{d_0}, \tag{1}$$

where d_{ij} is the spacing between the layers i and j, and d_0 is the ideal bulk interlayer distance of the substrate (1.91 Å). If there is some corrugation in the layer, we reference these numbers

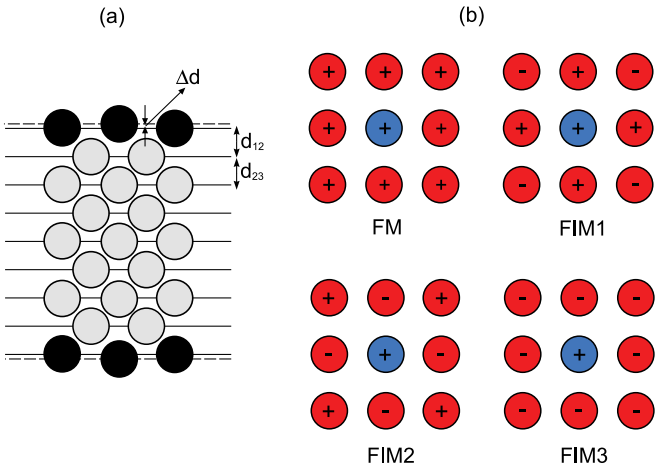

FIG. 1. (Color online) (a) Modeling of a symmetric film of 3*d* TM atoms (black) on a 7-layer Rh(001) substrate (gray). Indicated are the interlayer distances, d_{ij}, and the corrugation of the topmost layer, Δd, in the case of an alloy film. (b) Different magnetic structures of Fe_3Co or Co_3Fe alloys. Shown are the ferromagnetic (FM) and three possible ferrimagnetic (FIM) structures.

to the average atomic positions. The main results obtained from these investigations are presented in Fig. 2 and Table I. Figure 2 shows that in the case of ferromagnetic structures Δd_{12} is decreasing and Δd_{23} is increasing steadily with increasing the content of the cobalt, but for Δd_{23} the increase is small. In the case of AFM or ferrimagnetic (FIM) configurations there are slight oscillations in the relaxations Δd_{ij} with increasing cobalt content. Therefore, in the case of the magnetic ground state (refer next subsection), the relaxations show a maximum value of Δd_{12} and a minimum of Δd_{23} at the cobalt content of 0.5. These results match those reported in the literature for the pure Fe and Co films.[5]

The corrugation of the topmost layer, Δd_{FeCo}, in $Fe_{1-x}Co_x$ alloy film on Rh(001) was calculated. In ferromagnetically

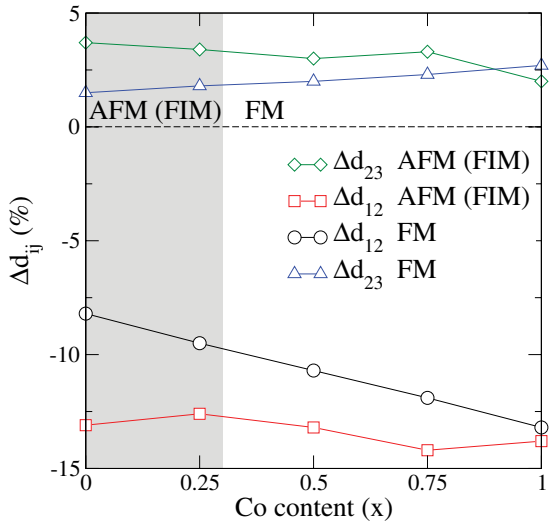

FIG. 2. (Color online) Relaxation of the topmost two layers Δd_{ij} of $Fe_{1-x}Co_x$/Rh(001) monolayer film as a function of Co content. For $x = 0.25$ and $x = 0.75$ the results for the FIM structures with lowest energies are shown.

ordered Fe_3Co and Co_3Fe the inequivalent Fe or Co atoms show very similar relaxations; therefore we can neglect the buckling between the inequivalent atoms. In these cases, Co shows a stronger inward relaxation than Fe, as can be expected from Δd_{12} in Fig. 2. We found the values of 0.014, 0.019, and 0.031 Å for the corrugation between Fe and Co in the structures Fe_3Co, FeCo, and Co_3Fe, respectively. In the case of AFM (FIM) structures, the situation is more complex. For example, for the ground state FIM1 of the Fe_3Co film (refer to the next subsection) we found a corrugation, $\Delta d_{\mathrm{Fe}\uparrow\mathrm{Fe}\downarrow}$, between the inequivalent Fe atoms of 0.056 Å, with the Fe atoms next to Co relaxed outwards. The nearest-neighbor Fe and Co atoms show almost the same relaxation; i.e., the minority spin Fe atom has the largest relaxation towards the substrate.

B. Magnetic order and moments

The magnetic order of the ground state is analyzed by determining the total energy difference between the AFM (FIM) and the FM configurations:

$$\Delta E = E_{\mathrm{AFM(FIM)}} - E_{\mathrm{FM}}. \quad (2)$$

Positive values indicate a FM ground state, while negative values denote AFM (FIM) order. To calculate this difference of energy, 78 $\mathbf{k}_\parallel$ points in the IBZ were used for the $c(2 \times 2)$ configuration and 36 $\mathbf{k}_\parallel$ points for the $p(2 \times 2)$ configuration. We found a FM ground state for Co, FeCo, and Co_3Fe and an AFM for Fe and (FIM) for Fe_3Co (Table I).

The density of state (DOS) is an important property to characterizing the stability of the magnetic structures. In a simple approximation, the stability of the magnetic structure of the film can be judged from a comparison of the DOS at the Fermi level (E_F) between the AFM (FIM) and the FM configurations: Larger values indicate less stability for a given magnetic state than smaller values. Figure 3 shows the DOS of the Fe, Co, and FeCo films on Rh(001), $n(E)$, in both FM and AFM configurations. Comparing the FM and AFM state we see from this figure that for Fe in the latter case the antibonding states are shifted farther away from the Fermi level than in the FM case. For the Co film, the opposite is true, while in the FeCo alloy similar peak positions are found. This indicates already a change from an AFM ground state in Fe to FM in Co films on Rh(001), as is indeed confirmed in Table I.

Let us now analyze the results of the local DOS (LDOS) in Fig. 4. The rhodium interface atom has an almost flat spectrum of density of states for all magnetic structures; i.e., its contribution to the total DOS at the Fermi level is small and constant in energy. Fe and Co atoms exhibit a LDOS for majority and minority states that is exchange split by about 3 to 4 eV depending on Fe and Co or depending on the antiferro- or ferromagnetic state. The exchange splitting is so large that the hybridization of the minority and the majority 3*d* states is different and the shift of the minority and majority states is not a rigid one, making an analysis of the magnetic ground state on the basis of the Stoner model difficult. The prominent features determining the magnetic ground state are the minority *d* states in the vicinity of about 1.5 eV above and below E_F, whose characteristic shape can be explained on the basis of a simple model build of two minority *d* states of a dimer hybridizing. In case of the FM state, both minority *d* states hybridize and form

TABLE I. Summary of the relaxations Δd_{ij}, magnetic moments m, and total energy differences $\Delta E = (E - E_{\mathrm{FM}})$ per TM atom results of iron, cobalt, and their alloys in different magnetic structures on rhodium (001) substrate. The structures FIM1 to FIM3 are shown schematically in Fig. 1.

		Δd_{12} (%)	Δd_{23} (%)	m_{Fe} (μ_{B})	m_{Co} (μ_{B})	$m_{\mathrm{Rh(I)}}$ (μ_{B})	ΔE (meV)
Fe	FM	− 8.2	1.5	2.99		0.24	
	AFM	− 13.1	3.7	2.93		0.00	− 59.9
Co	FM	− 13.2	2.7		2.03	0.48	
	AFM	− 13.8	2.0		1.72	0.00	161.2
FeCo	FM	− 10.7	2.0	3.08	1.91	0.34	
	FIM	− 13.2	3.0	2.97	− 1.69	− 0.07	81.9
Fe_3Co				2.99			0.0
	FM	− 9.5	1.8	3.04	1.89	0.29	
				− 2.95			− 25.5
	FIM1	− 12.6	3.4	2.95	1.79	0.12	
				2.97			15.8
	FIM2	− 13.3	3.7	− 2.95	1.71	0.03	
				− 2.99			55.5
	FIM3	− 11.7	3.1	− 2.94	1.49	0.14	
Co_3Fe					2.01		0.0
	FM	− 11.9	2.3	3.08	1.97	0.39	
					− 1.71		80.3
	FIM1	− 12.7	2.4	3.06	1.77	0.16	
					1.74		119.2
	FIM2	− 13.7	2.7	3.03	− 1.68	− 0.01	
					− 1.96		41.0
	FIM3	− 14.2	3.3	3.00	− 1.80	− 0.22	

minority bonding and antibonding states as can be seen in the LDOS. The hybridization leads to a broadening of the *d* states and maximum energy is gained if the bonding state is filled, which is about the case for the ferromagnetic Co monolayer on Rh(100). Comparison of the minority *d* states in Fe and Co shows that the increased *d*-band filling shifts the Co states to lower energies.

In the case of the FeCo alloy, hybridization between the Fe and Co *d* states leads to bonding states that are of Co character and antibonding states of Fe character. For the FM structures, we note that there are two broad peaks in the minority spin local density of states for both iron and cobalt within about 1.5 eV above and below E_{F}. In case of nearest-neighbor antiferromagnetic order (FIM2, FIM3, AFM states of Fe and Co) the minority *d* state of atom 1 is in the same spin channel

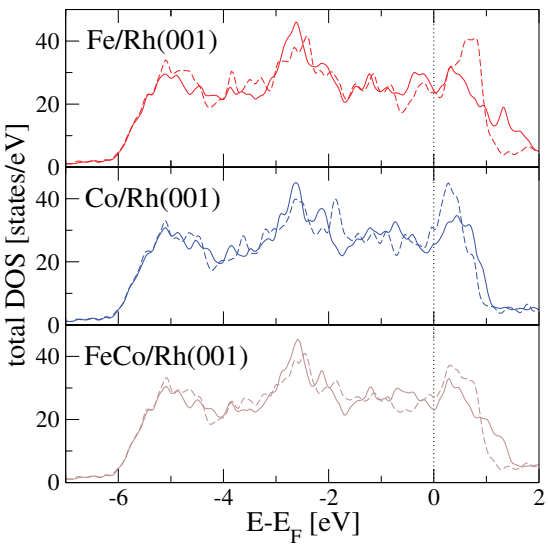

FIG. 3. (Color online) Total, spin integrated density of states (DOS) in $Fe_{1-x}Co_x$ alloy films on Rh(001) for $x = 0.0$, 1.0, and 0.5 in the FM (full line) and AFM (dashed line) state.

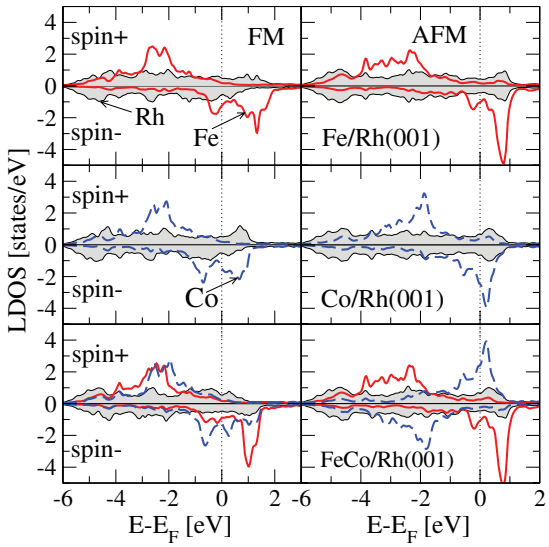

FIG. 4. (Color online) LDOS for the Fe (full red line), Co (dashed blue line), and Rh (gray shaded area) interface atoms in the FM and AFM (FIM) configurations of Fe, Co, and FeCo on Rh(001) surface.

as the majority d state of atom 2, which is 3–4 eV lower in energy. Since the energetic overlap is small, the LDOS remains narrower than in the FM state. Thus, in the case of the AFM structures, we observe sharp peaks of the Fe and Co LDOS in the unoccupied part and a rather broad feature in the occupied region.

Both for Co and FeCo we can see that the large DOS at E_F is induced by the Co minority states, destabilizing the AFM state. In the FM state of Co, the broadening is due to the orbital hybridization of the 3d atoms. For the FeCo alloy, the situation is somewhat different. In this case the orbital hybridization leads to the formation of a sharp peak superimposed on a broad peak in the minority spin LDOS for each 3d atom. This is due to the fact that the orbitals in the iron or the cobalt are not within the same energy levels.

For Fe, the Fermi level is always in a minimum of the LDOS; therefore the local magnetic moments in the FM and AFM states are almost identical [Fig. 5(b)]. The Co moment is slightly reduced in the AFM (FIM) states, since E_F is shifted into the peak of the Co minority LDOS. Figure 5 shows that m_{3d} is almost constant with increasing cobalt content (x) in the cases of both the FM and the AFM (FIM) configurations,

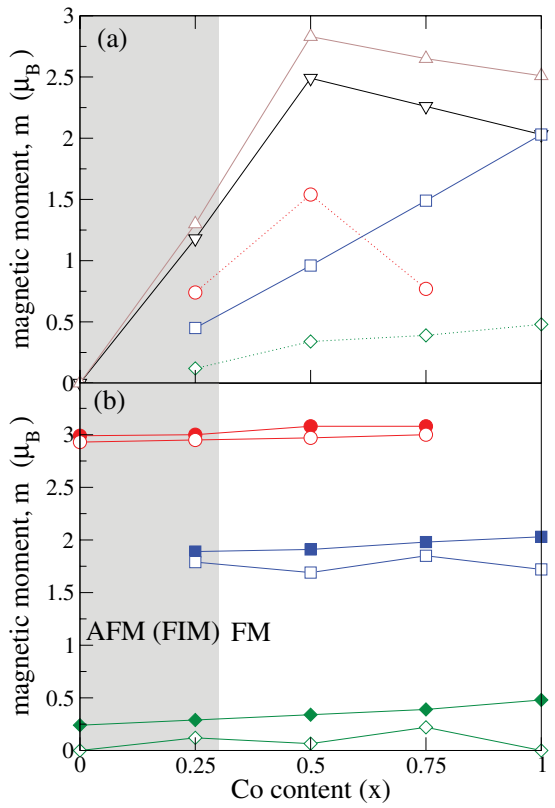

FIG. 5. (Color online) (a) Different atom-resolved contributions in the total magnetic moment of $Fe_{1-x}Co_x$/Rh(001) film as function of Co content (GS state). Triangle down: $(1-x)m_{Fe} + x\,m_{Co}$, circle: $(1-x)m_{Fe}$, square: $x\,m_{Co}$, diamond: m_{Rh}, and triangle up: m_{tot}. (b) Absolute value of the magnetic moments of the 3d TMs and the interface Rh moments of $Fe_{1-x}Co_x$/Rh(001) monolayer film as a function of Co content [FM and AFM (FIM) states]. Circle: m_{Fe}, square: m_{Co}, diamond: $m_{Rh(I)}$, full: FM, and open: AFM (FIM). The gray shaded area marks concentration region where AFM (FIM) structures are the ground state.

while $m_{Rh(I)}$ is steadily increasing with x in the case of the FM configuration. Furthermore, we note that the ratio m_{Fe}/m_{Co} is of about 1.5 and this value is in agreement with the observed value (1.4) that reported in Ref. 2. Figure 5(a) shows that the total magnetic moment has a maximum value of 2.8 μ_B/atom at the cobalt content of $x = 0.5$ (FeCo). From these figure we note that the magnetic moment has the same trend for bulk alloys as reported in Ref. 18; i.e., the highest magnetic magnetic moments are observed in the Co-rich alloys around $x = 0.6$.

Since the magnetic moments are rather constant, one can apply the classical Heisenberg model of magnetism in order to analyze the magnetic order from the results of DFT. The corresponding Hamiltonian describes the interaction between two spins $\vec{S}$ at sites i and j in the form

$$H_{ex} = -\sum_{ij} J_{ij}\,\vec{S}_i \cdot \vec{S}_j, \tag{3}$$

where J_{ij} is the exchange coupling constant between the two spins. The sign of J_{ij} determines whether a parallel (FM, $J_{ij} > 0$) or antiparallel (AFM, $J_{ij} < 0$) alignment of $\vec{S}_i$ and $\vec{S}_j$ is preferred. This can be used as a phenomenological starting point in the investigation of the magnetic order in a crystal. Although the Heisenberg model was introduced originally for magnetic insulators with localized moments, it can be applied to metallic systems under certain conditions. Assuming that the exchange interactions do not differ significantly for different concentrations x, the J_{ij}'s can be estimated from the energy differences listed in Table I. These exchange constants for the $Fe_{1-x}Co_x$ monolayers on Rh(001) are denoted as $J_n^{\nu\nu'}$ where ν and ν' are atom types and $n = 1$ characterizes nearest-neighbor interactions, while $n = 2$ stands for next-nearest-neighbor interactions. Applying this model to FM and AFM structures with $x = 0$,0.5, and 1 leads to the values of the nearest-neighbor exchange interaction constants: $J_1^{FeFe} = -1.67$ meV/μ_B^2, $J_1^{CoCo} = 11.12$ meV/μ_B^2, and $J_1^{FeCo} = 4.05$ meV/μ_B^2. Comparing FM and FIM structures for $x = 0.25$ and 0.75 allows us to estimate also $J_2^{FeCo} = 0.04$ meV/μ_B^2. We note here that the contribution of the next-nearest neighbors to the exchange interactions is already small and probably within the limit of accuracy of the model; therefore we consider only interactions between the nearest neighbors. It is known that these metallic alloys can be ordered at random and for each chemical structure there are a several possible configurations of the magnetic arrangements. The Heisenberg model allows us to predict which of the magnetic structures is more stable. For example, the Heisenberg J's allow us to predict the magnetic ground state of the $p(2 \times 2)$ Fe_3Co alloy from the nearest-neighbor exchange constants obtained from the $Fe_{1-x}Co_x$ structures for $x = 0$, 0.5, and 1: From the Heisenberg model we expect the FIM1 structure to be most stable, 28.7 meV lower than the FM state. This is in agreement with the result from Table I, where 25.5 meV was found.

Through this model one can also study the magnetic ground state for more complex alloy configurations on a square lattice. In our case there are three nearest-neighbor bonds which can be formed for different configurations of the $Fe_{1-x}Co_x$ alloy monolayer on Rh(001). The combination of these pairs leads to

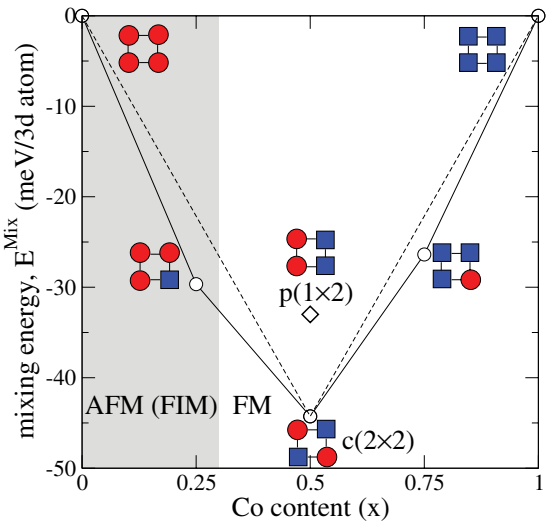

FIG. 6. (Color online) Mixing energies of ferromagnetic $Fe_{1-x}Co_x$ alloy monolayers on Rh(001). Open symbols are DFT results, the dashed line denotes expectation from a pair approximation, the full line corresponds to an approximation using four-atom clusters (see text).

the formation of six configurations that the two atom types can assume in a square, $p(2 \times 2)$ unit cell (see Fig. 6). Five of these arrangements we encountered already in our studies of the exchange interaction as discussed above. Another possibility, a $p(1 \times 2)$ row-wise-ordered structure, will be considered in the following. Although we limit ourselves to ordered structures, in principle also disordered alloys can be taken into account. Using DFT with the coherent potential approximation (CPA), Abrikosov and co-workers considered the possible formation of random FeCo alloys for the bulk phases. It has been found that partially ordered B2 structures form the ground state over a wide concentration range. The connection to magnetism was established by a canonical d-band model. It is quite probable that a similar mechanism also stabilizes ordered phases in low-dimensional FeCo alloys.

The mixing energy can be calculated for the binary configurations, which measures the energetic stability of the heterogeneous system described by a given composition with respect to a superposition of the systems with different compositions. For a certain N-atom configuration (or cluster), it is defined as the energy difference with respect to homoatomic N-atom configurations. The mixing energy per atom of a bimetallic system is then given by

$$E^{\mathrm{Mix}} = \frac{1}{N}\left[E_{A_n B_{(N-n)}} - \frac{n}{N}E_{A_N} - \frac{(N-n)}{N}E_{B_N}\right], \qquad (4)$$

where A and B are the different species of atoms in the N-atom configuration and n denotes the number of atoms of species A. Furthermore $E_{A_n B_{(N-n)}}$ is the total energy of the bimetallic system, while E_{A_N} and E_{B_N} are the total electronic energies of the pure metals A_N and B_N, respectively. The results of the calculations of mixing energy are presented in Fig. 6. We note that an approximation using $p(2 \times 2)$ configurations (four-atom clusters) leads to a further stabilization of the ordered structures for $x = 0.25$ and $x = 0.75$ as compared to the pair approximation constructed from the $c(2 \times 2)$ FeCo alloy. Negative values of E^{Mix} indicate that the $p(1 \times 2)$ row-wise-ordered structure is stable, although E^{Mix} tends to maximize A-B pairs and therefore the $c(2 \times 2)$ structure is more stable.

From the Heisenberg model we know that positive values of J_1^{FeCo} with $|J_1^{\mathrm{FeFe}}| < |J_1^{\mathrm{FeCo}}|$ lead to a ferromagnetic order of the $p(1 \times 2)$ structure. In this model the $p(1 \times 2)$ configuration in the FM order is 7.3 meV/atom lower in energy than a state with an antiferromagnetic Fe configuration. In summary, we can expect a wide range of concentrations, where the FM state is the ground state.

C. Magnetic anisotropy and orbital moments

The magnetic anisotropy is one of the most important intrinsic quantities in particular with respect to applications of thin films and multilayers. It allows us to determine the magnetization direction (in-plane or out-of-plane) of the magnetic system, and also to determine its critical temperature in two dimensions, T_2, as the magnetic anisotropy is the decisive quantity rising T_2 to a finite value by stabilizing a 2D magnet against thermal fluctuations. In principle, two terms contribute to the magnetic anisotropy energy (MAE): the dipole-dipole interaction, leading in a ferromagnetic system with some boundaries to the magnetic shape anisotropy (MSA), and the spin-orbit coupling term giving the dominant contribution to the magnetocrystalline anisotropy (MCA).

The MCA is determined by calculations including spin-orbit coupling (SOC) and applying the force theorem.[19] Then, the MCA is given by the difference of the single-particle energies of all occupied states between the magnetic states of in-plane (010) and out-of-plane (001) magnetization:

$$K_{\mathrm{MCA}} = \sum_{\vec{k},\nu} \varepsilon_{\parallel}(\vec{k},\nu) - \sum_{\vec{k},\nu} \varepsilon_{\perp}(\vec{k},\nu), \qquad (5)$$

where $\varepsilon_{\parallel}$ and $\varepsilon_{\perp}$ denote the eigenvalues for in-plane and out-of-plane magnetization, respectively. Positive values indicate that the out-of-plane direction is more stable. For the calculations of the MCA 1296 $\mathbf{k}_{\parallel}$ points were used in the full 2D BZ. The results are illustrated in Table II and Fig. 7. Considering only the ground-state magnetic structure an out-of-plane anisotropy in $Fe_{1-x}Co_x$/Rh(001) was predicted for $x = 0.5$ and 0.75 and in-plane for $x = 0, 0.25$, and 1. It is clear from these results that the general trend of the magnetic anisotropy is the following: As a function of band filling (increasing x) the anisotropy of the FM phase changes smoothly from out-of-plane to in-plane. Although antiferromagnetic structures are always in-plane magnetized, the changes of the MAE with x shows the same trend as the FM case. In total, we observe an in-plane anisotropy in $Fe_{1-x}Co_x$ for $0 < x < 0.3$ and $x > 0.8$ and an out-of-plane anisotropy for $0.3 < x < 0.8$. These results are in good agreement with those for thicker FeCo films that have been reported in Ref. 2.

Typically, in ultrathin magnetic films the contribution of the MCA to the magnetic anisotropy energy is larger than that of the shape anisotropy. The MSA is the consequence of the anisotropy of the dipole-dipole interaction: For FM ordering the shape anisotropy K_{shape} (in Hartree atomic units) of a perfectly flat film of infinite extension is given by the local

TABLE II. The magnetocrystalline anisotropy, K_{MCA}, per $3d$ atom and the orbital moment anisotropy (OMA) results of iron, cobalt, and their alloys on rhodium (001) substrate. Positive (negative) values of the MCA signify an out-of-plane (in-plane) magnetization.

		K_{MCA} (meV)	$\mathrm{OMA_{Fe}}$ (μ_{B})	$\mathrm{OMA_{Co}}$ (μ_{B})	$\mathrm{OMA_{Rh}^{tot}}$ (μ_{B})	$\mathrm{OMA_{tot}}$ (μ_{B})
Fe	FM	0.29	0.003		−0.008	−0.005
	AFM	−0.09	0.001		−0.002	−0.001
Co	FM	−0.10		0.040	0.009	0.049
	AFM	−0.53		0.054	0.005	0.058
FeCo	FM	0.25	0.001	0.025	0.003	0.015
	FIM	−0.25	0.005	0.052	0.001	0.029
Fe_3Co	FIM1	−0.14	0.007	0.028	0.001	0.009
			−0.001			
Co_3Fe	FM	0.09	−0.003	0.034	0.006	0.029
				0.030		

magnetic moment m (in μ_{B}) and the atomic volume V as[20]

$$K_{\mathrm{shape}} = -\frac{\pi}{c^2}\frac{m^2}{V}, \tag{6}$$

where the negative sign indicates that an in-plane easy axis is favored. In very thin films an approximation of the dipole-dipole interaction by this continuum approach is problematic and it is preferable to carry out the dipole sum explicitly. This is also necessary for AFM films, where a slight preference for the out-of-plane direction is found.[21]

Since there are only two systems with an out-of-plane easy axis in the ground state, FeCo and Co_3Fe, we can focus on these two. In our calculations of the dipole-dipole interaction, including also the induced magnetic moments of the substrate, we find values of $K_{\mathrm{dip}} = -0.12$ meV and -0.10 meV per atom for the two systems, respectively. These values show that the FeCo alloy maintains its out-of-plane easy axis, while Co_3Fe has an almost vanishing total anisotropy.

The orbital moment anisotropy (OMA) is defined as the difference of the orbital moment, m_l, when the magnetization points along the in-plane (010) and out-of-plane (001) directions, respectively:

$$\mathrm{OMA} = m_l^{\parallel} - m_l^{\perp}. \tag{7}$$

Figure 8(a) represents the OMA as a function of the cobalt content. It is clear that the main contributions to the total orbital moment is due to the cobalt and iron atoms [Fig. 8(b)], but also the Rh atoms give a positive contribution starting from a certain point (at the cobalt content of 0.3) where the magnetic phase of the $Fe_{1-x}Co_x$ alloy monolayer becomes ferromagnetically ordered.

Following the model of Bruno,[22] the anisotropy of the orbital moment is closely related to the magnetocrystalline anisotropy when the exchange splitting is large and separates majority and minority bands of the magnetic material. This relation can be expressed as

$$K_{\mathrm{MCA}} = -\frac{\xi}{4\mu_{\mathrm{B}}}(m_l^{\parallel} - m_l^{\perp}) = -\frac{\xi}{4\mu_{\mathrm{B}}}\mathrm{OMA}, \tag{8}$$

where the spin-orbit coupling constant ξ is on the order of 50–100 meV for $3d$ metals. This model suggests that in the present case there is a competition in order to establish either an easy axis perpendicular or parallel to the film plane, the cobalt OMA favoring an in-plane anisotropy, while in Fe the OMA is tiny and for most concentrations in favor of an out-of-plane easy axis direction.

From Fig. 7 we concluded the following trend for the MCA: The monolayer film has a perpendicular magnetic anisotropy within the whole region of ferromagnetic phase, except close to the pure Co phase, while a parallel magnetic anisotropy is observed in the whole region of antiferromagnetic and ferrimagnetic phases without exception. The results of Table II show that although there is no agreement with the Bruno model in predicted magnetization directions, the trends are mainly reproduced, i.e., larger (positive) OMA leads to a tendency towards in-plane magnetization.

In the simple model of Eq. (8) the large OMA found for Co completely dominates the contributions to the MAE, suggesting an in-plane easy axis over almost the whole concentration range, which is not observed. Also the inclusion of the Rh with its larger spin-orbit coupling constant and the

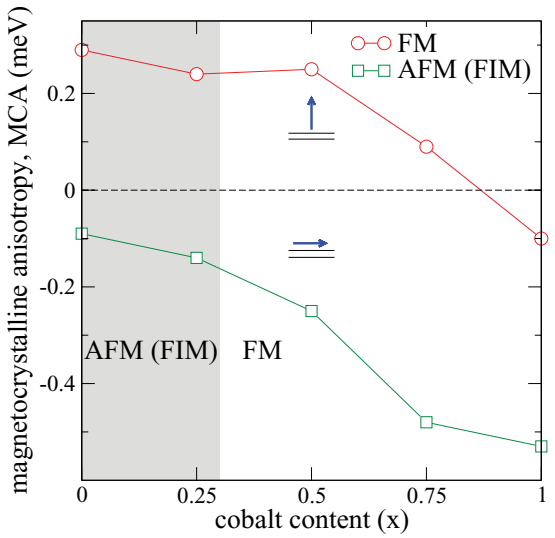

FIG. 7. (Color online) Magnetocrystalline anisotropy of $Fe_{1-x}Co_x$/Rh(001) monolayer films as a function of Co content [FM and AFM (FIM) states].

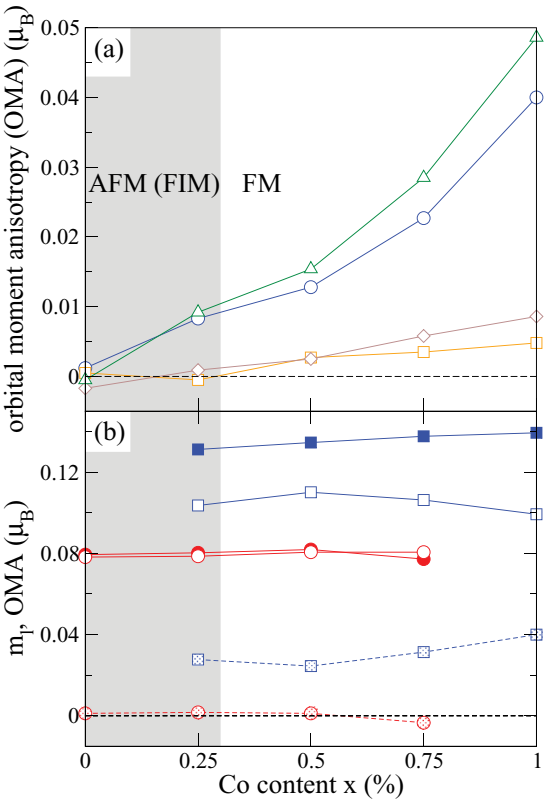

FIG. 8. (Color online) (a) Different atom-resolved contributions to the orbital moment anisotropy (OMA) of $Fe_{1-x}Co_x$/Rh(001) as function of the Co content (values for ground-state magnetic structures). Circle: $(1-x)\mathrm{OMA_{Fe}} + x\,\mathrm{OMA_{Co}}$, square: $\mathrm{OMA_{Rh(I)}}$, diamond: $\sum \mathrm{OMA_{Rh}}$, and triangle up: $\mathrm{OMA_{tot}}$. (b) Orbital moments m_l and OMA of Fe (red circles) and Co (blue squares) atoms in $Fe_{1-x}Co_x$/Rh(001) monolayer film as a function of Co content. Full and open symbols are $m_l^{\parallel}$ and $m_l^{\perp}$, respectively, and shaded symbols indicate the OMA.

OMA shown in Fig. 8(a) in this relation does not change the trend, although the presence of Rh is probably responsible for strong spin-mixing contributions to the anisotropy[23] and the obvious deviations from the simple relation given by Eq. (8).

In two-dimensional systems the magnetic anisotropy is of particular importance for the stabilization of the magnetic order at finite temperatures. For example, in a system with uniaxial anisotropy it was shown that the ordering temperature in two dimensions, T_2, can be derived by a renormalization of the ordering temperature in three dimensions, T_3, according to[24]

$$T_2 = \frac{2T_3}{\ln(\pi^2 J/K)}, \tag{9}$$

where J is the nearest-neighbor exchange coupling as defined in a Heisenberg model and K is the uniaxial anisotropy. For a square lattice with out-of-plane anisotropy, this model can be used to estimate the ordering temperature from the energy difference between FM and AFM structures and the anisotropy. Since the $Fe_{1-x}Co_x$ alloy films show a strong out-of-plane anisotropy in the ground state with a maximum at $x = 0.5$, we can focus on the FeCo film. Using the calculated value of the ordering temperature of an ordered FeCo alloy of cubic symmetry in three dimensions,[25] we find a value of 482 K for the ordering temperature of the FeCo film. Also experimentally for thicker films ordering temperatures above room temperature are found.

IV. SUMMARY

Ultrathin monolayer films of ordered $Fe_{1-x}Co_x$ (with $x = 0.0$, 0.25, 0.5, 0.75, and 1.0) were studied on top of Rh(001) surface including relaxations of the topmost layers. The full-potential linearized augmented plane wave method (FLAPW) was used to investigate the main magnetic properties of these magnetic ultrathin alloy films. The magnetic order was found to be FM for Co, FeCo, and Co_3Fe overlayers, while Fe and Fe_3Co favor an AFM (FIM) ground state. Calculations of the magnetic anisotropy showed that only FeCo and Co_3Fe monolayers on Rh(001) have an out-of-plane easy axis in their ground state, while the magnetization of Fe, Co, and Fe_3Co is in-plane oriented. Thus, FeCo/Rh(100) combines many favorable properties: For this system we found the largest magnetic moment; it is ferromagnetic; it has the largest out-of-plane anisotropy, a very high Curie temperature, and a large heat of formation. We investigated ordered compounds. For a Co concentration larger than 25%, we do not expect large changes in the total moment in the case of disorder, but we think that the degree of disorder may alter the magnetic anisotropy and thus will influence the Curie temperature. The observed properties make these ultrathin films useful materials for magnetic recording applications.

ACKNOWLEDGMENTS

Helpful discussions with D. Wortmann are gratefully acknowledged. Furthermore, S. Blizak acknowledges financial support from the Algerian ministry of higher education and scientific research.

*Present Address: Peter Grünberg Institut and Institute for Advanced Simulation, Forschungszentrum Jülich and JARA, 52425 Jülich, Germany.
†g.bihlmayer@fz-juelich.de

[1] S. Thompson, J. Phys. D **41**, 093001 (2008).
[2] F. Yildiz, F. Luo, C. Tieg, R. M. Abrudan, X. L. Fu, A. Winkelmann, M. Przybylski, and J. Kirschner, Phys. Rev. Lett. **100**, 037205 (2008).
[3] F. Yildiz, M. Przybylski, and J. Kirschner, Phys. Rev. Lett. **103**, 147203 (2009).
[4] F. Yildiz, M. Przybylski, X. D. Ma, and J. Kirschner, Phys. Rev. B **80**, 064415 (2009).
[5] A. Al-Zubi, G. Bihlmayer, and S. Blügel, Phys. Rev. B **83**, 024407 (2011).
[6] I. A. Abrikosov, P. James, O. Eriksson, P. Söderlind, A. V. Ruban, H. L. Skriver, and B. Johansson, Phys. Rev. B **54**, 3380 (1996).

[7]M. Friák, M. Šob, and V. Vitek, Phys. Rev. B **63**, 052405 (2001).
[8]D. Spišák and J. Hafner, Phys. Rev. B **73**, 155428 (2006).
[9]T. Burkert, L. Nordström, O. Eriksson, and O. Heinonen, Phys. Rev. Lett. **93**, 027203 (2004).
[10]P. Hohenberg and W. Kohn, Phys. Rev. **136**, B864 (1964).
[11]W. Kohn and L. J. Sham, Phys. Rev. **140**, A1133 (1965).
[12]U. Barth and L. Hedin, J. Phys. C **5**, 1629 (1972).
[13] FLEUR, http://www.flapw.de/.
[14]E. Wimmer, H. Krakauer, M. Weinert, and A. J. Freeman, Phys. Rev. B **24**, 864 (1981).
[15]H. Krakauer, M. Posternak, and A. J. Freeman, Phys. Rev. B **19**, 1706 (1979).
[16]J. P. Perdew, K. Burke, and M. Ernzerhof, Phys. Rev. Lett. **77**, 3865 (1996).
[17]C. Li, A. J. Freeman, H. J. F. Jansen, and C. L. Fu, Phys. Rev. B **42**, 5433 (1990).
[18]A. Diaz-Ortiz, R. Drautz, M. Fähnle, H. Dosch, and J. M. Sanchez, Phys. Rev. B **73**, 224208 (2006).
[19]A. R. Mackintosh and O. K. Andersen, in *Electrons at the Fermi surface*, edited by M. Springford (Cambridge Univ., London, 1980), p. 149.
[20]S. Blügel and G. Bihlmayer, in *Handbook of Magnetism and Advanced Magnetic Materials*, edited by H. Kronmüller and S. Parkin (J. Wiley & Sons, Ltd., Chichester, UK, 2007), Vol. 1.18.
[21]P. J. Jensen, Acta Phys. Pol. A **92**, 427 (1997).
[22]P. Bruno, Phys. Rev. B **39**, 865 (1989).
[23]G. van der Laan, J. Phys.: Condens. Matter **10**, 3239 (1998).
[24]R. P. Erickson and D. L. Mills, Phys. Rev. B **43**, 11527 (1991).
[25]M. Lezaic, P. Mavropoulos, and S. Blügel, Appl. Phys. Lett. **90**, 082504 (2007).